



## **Investigation of Stiffener Requirements in Castellated Beams**

Fatmir Menkulasi<sup>1</sup>, Cristopher D. Moen<sup>2</sup>, Matthew R. Eatherton<sup>3</sup>, Dinesha Kuruppuarachchi<sup>4</sup>

### **Abstract**

This paper presents an analytical investigation on the necessity of stiffeners in castellated beams subject to concentrated loads. Several castellated beams, with and without stiffeners, and with various depths are investigated using non-linear finite element analysis to examine their behavior to failure when subject to concentrated loads. The efficiency of stiffeners to increase the resistance of castellated beams against concentrated loads is examined. The concentrated loads are applied at the center of the full height web, at the center of the opening and between the web and the opening to cover the potential range of the concentrated force location. For each investigated beam depth and stiffener arrangement, the loads that cause failure are noted. In addition, a simplified approach for checking the limit state of web post buckling in compression is proposed and recommendations on the necessity of stiffeners are presented.

---

<sup>1</sup>Assistant Professor, Department of Civil Engineering, Louisiana Tech University, Ruston, LA  
<fmenkula@latech.edu>

<sup>2</sup> Associate Professor, Department of Civil & Environmental Engineering, Virginia Tech, Blacksburg, VA  
<cmoen@vt.edu>

<sup>3</sup> Assistant Professor, Department of Civil & Environmental Engineering, Virginia Tech, Blacksburg, VA  
<meather@vt.edu>

<sup>4</sup>Undergraduate Research Assistant, Department of Civil Engineering, Louisiana Tech University, Ruston, LA  
<dku003@latech.edu>

## 1. Introduction

Castellated beams have been used since the 1940's (Zaarour and Redwood 1996) because of their ability to offer wide and open spaces, reduce floor to floor heights, increase illumination and improve aesthetic appeal. Engineering advantages of castellated beams include superior load deflection characteristics, higher strength and stiffness, lower weight and the ability to span up to 90 ft without field splicing. Also, the automation process has reduced the cost of their fabrication to the level where for certain applications they may be competitive with open web steel joists (Zaarour and Redwood 1996). Castellated beams have consisted typically of hexagonal or octagonal openings, with the octagonal openings made possible by the addition of incremental plates between the cut webs. Figure 1 illustrates an application of castellated beams with hexagonal openings. Another similar form are cellular beams, which consist of circular web openings. Cellular beams have gained popularity because of the aesthetic appeal they offer in architecturally exposed surfaces. Some manufacturers have recently developed new opening shapes for castellated beams. For example ArcelorMittal presented castellated beams with sinusoidal web openings, named as the Angelina Beam (Wang et al. 2014). Durif and Bouchair (2013) performed an experimental study on beams with such openings. Tsavdaridis and D'Mello (2012;2011) investigated the behavior of castellated beams with novel elliptically based web openings.



Figure 1. Application of castellated beams (Scherer Steel Structures, Inc.)

Castellated beams are subject to a variety of failure modes. Some of the typically investigated failure modes are: flexural failure (Figure 2), shear failure, lateral-torsional buckling (Figure 3), Vierendeel mechanism (Figure 4), web post buckling or yielding (Figure 5), local buckling and welded joint rupture (Figure 6). Pure bending, shear and overall lateral-torsional buckling are similar to the corresponding modes for solid-web beams and can be treated in an almost identical manner, if the relevant geometric properties used are based on the reduced cross-section (Soltani et al. 2012). The failure modes that are specific to castellated beams are the Vierendeel mechanism, yielding or buckling of the web post and fracture of the welded joint. Vierendeel mechanism is likely to occur in castellated beams with large web opening lengths under high shear to moment ratio. This failure mode is manifested by the formation of four plastic hinges in the upper and lower T-section due the combination of the global moment and Vierendeel moment. The Vierendeel moment forms due to the transfer of the shear forces across the opening. Buckling of the web post can occur due to shear or compression. The buckling or yielding of the web post in shear occurs due to the combination of the shear force acting at mid-depth of the web post with a double curvature bending moment over the height of the web post. The buckling of the web post in compression can occur when the web post is subject to concentrated forces. The horizontal shear force can also cause the fracture of the welded joint in the web post, especially in cases when the length of the welded joint is small. Local buckling may occur in three ways in castellated beams:

1) buckling of the compression flange, 2) buckling of the T-section in compression, and 3) vertical instability of the sides of the web openings in high shear zones. Ellobody (2011;2012) reports that additional failure modes may occur independently or interact with each other.

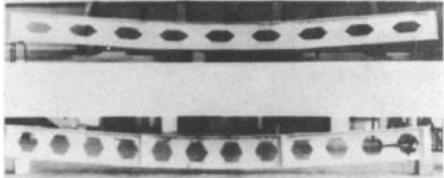


Figure 2: Laterally braced flexural failure (Halleux 1967)

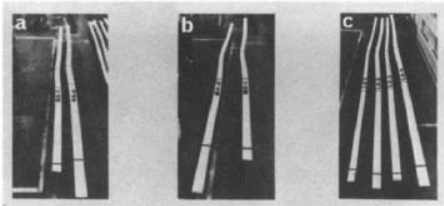


Figure 3: Lateral-torsional buckling (Nethercot and Kerdal 1982)

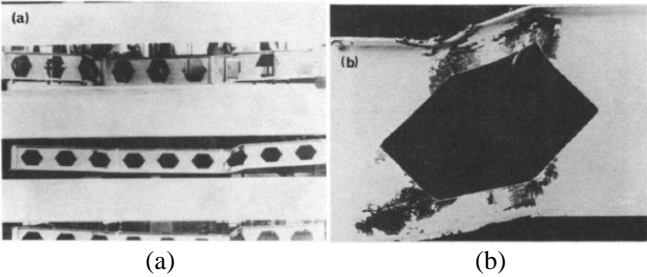


Figure 4: Vierendeel mechanism caused by shear transfer through perforated web zone (Halleux 1967), (a) overall view, (b) close-up view of castellation

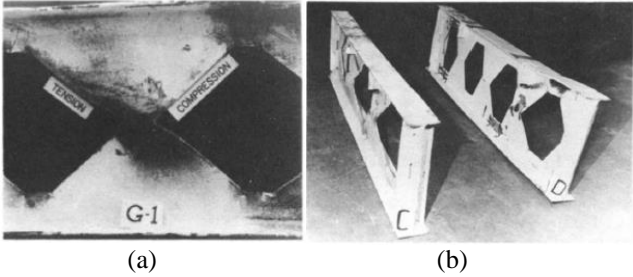


Figure 5: Web buckling (a) shear compressive half-wave near a support; (b) flexural buckling below a concentrated load (Hosain and Spiers 1973)

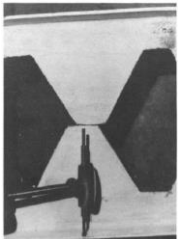


Figure 6: Rupture of a welded joint (Halleux 1967)

In many cases, castellated beams are subject to concentrated loads, such as a reaction from a column or a reaction from a supporting girder. The solution in situations like this is typically to provide a stiffener or filler plate at such concentrated load locations to prevent the buckling of the web post due to compression. However, both of these solutions require additional labor and in the case of the filler plate may defeat the aesthetic appeal offered by castellated beams. Additionally, if the advantages of automation are to be fully exploited such strengthening details must be minimized. The purpose of this paper is to twofold: a) to investigate the capacity of castellated beams subject to concentrated loads by determining the loads that cause the buckling of the web, and b) to quantify the enhanced capacity of the castellated beams against concentrated loads when stiffeners are provided. This is accomplished by performing 30 nonlinear finite element analyses, which feature various locations of the concentrated force, castellated beams with and without stiffeners and various web post height to thickness ratios. In this study only castellated beams with hexagonal openings are investigated. A simplified approach, utilizing an effective web width is proposed to aid engineers during the design process.

## 2. Design Methods

At present, there is not a generally accepted design method published in the form of a design guide for castellated beams primarily because of the complexity of their behavior and the associated modes of failure. Soltani et al. (2012) report that at European level, design guidance given in the annex N of ENV 1993-1-1 was prepared in draft format but was never completed (RT959 2006). In the United States, while Steel Design Guide 2 (Darwin 2003) covers steel and composite beams with web openings, it is explicitly stated that castellated beams are excluded. Various design approaches exist for how to treat failure modes such as Vierendeel mechanism, fracture of welded joint, and web-post buckling due to the horizontal shear and bending moments. Soltani et al. (2012) provide a summary of these design methods and propose a numerical model to predict the behavior of castellated beams with hexagonal and octagonal openings up to failure. Tsavdaridis and D'Mello (2012; 2011) performed an optimization study on perforated steel beams with various novel web opening shapes through non-linear finite element analyses and an investigation on the behavior of perforated steel beams with closely spaced web openings. Zaarour and Redwood (1996) investigated the strength of castellated beams susceptible to web-post buckling due to horizontal shear and bending moments. Wang et al. (2014) examined the Vierendeel mechanism failure of castellated beams with fillet corner web openings.

One of the studies that addresses the resistance of castellated beams against concentrated loads, in addition to the other modes of failure, is the one performed by Hosain and Speirs (1973), in which they tested 12 castellated beams with the objective of investigating the effect of hole geometry on the mode of failure and ultimate strength of such beams. An attempt was made to study the phenomenon of web buckling due to compression and due to shear in the framework of existing approximate design methods of that time. Three beams failed prematurely due to web buckling and they either had no stiffeners or partial depth stiffeners below the concentrated loads. Buckling of the web posts prevented these beams from reaching their maximum capacity. The method proposed by Blodgett (1966) was used to compare the predicted capacity of the web post in compression with the experimentally obtained failure loads. Blodgett's method treats the non-prismatic solid web as a column having a length equal to the clear height of the hole, a width equal to the web weld length and a thickness equal to the web thickness (Figure 7). To calculate the effective column length ( $kl/r$ ),  $k$  was assumed to be 1.0.

Kerdal and Nethercot (1984) reviewed previous studies on the structural behavior of castellated beams and identified a number of different possible failure modes. It was concluded that both lateral-torsional instability and the formation of a flexural mechanism may be handled by an adaption of established methods for plain webbed beams, provided that the cross-sectional properties are those corresponding to the centerline of a castellation. It was also concluded that the methods available at that time for the determination of collapse in the other modes, while rather less accurate, were adequate for design except in the case of web post buckling in compression. Kerdal and Nethercot (1984) state that while the web post could be considered to be a column having the depth of the hole and the area of the welded joint, there does not seem to be an agreement as to which effective length of the column to use. For example, an effective length factor of 0.75 was used in the study by the United Steel Co. Ltd. (1957). This was later (1962) reduced to 0.5 in a report by the same agency. Finally, Hosain and Speirs (1973) assumed the web posts to be pinned at both ends. Accordingly, one of the conclusions in the report by Kerdal and Nethercot (1984) is that no satisfactory method has been identified for the prediction of the load causing vertical buckling of the web post under a concentrated load or at a reaction point. As a result, this failure mode was reported as an area of uncertainty in the design of castellated beams and there is a need to obtain a better idea as to what is the effective area of the column and its effective length.

In the light of this discussion, the investigation described in this paper was undertaken with the goal of investigating the capacity of castellated beams under concentrated loads using nonlinear finite element analysis and models that specifically address this condition by isolating the beam sections from the other modes of failure.

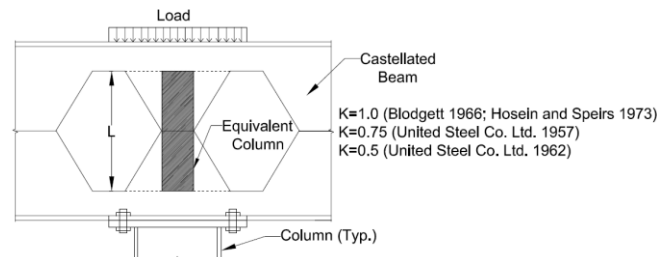


Figure 7: Simplified equivalent column approach for the investigation of the limit state of web post buckling in compression

### 3. Research Approach

To investigate the capacity of castellated beams when they are subject to concentrated loads five beam depths were selected (Table 1). Next to each castellated beam section is provided the original wide flange beam used to fabricate the castellated beams. These beams were selected such that they covered a wide range of depths, so that the capacity of each section against concentrated loads, with and without stiffeners, could be investigated. In cases when castellated beam sections feature stiffeners, the thickness of the stiffener was always 0.5 in. The web clear height to thickness ratios for these five beams range from 25.6 to 86.6. Table 2 provides a summary of the information used to define the geometry of the castellated beams. Each beam depth was subject to compressive loads at the top flange (Figure 8). The compression load was applied in the form of a uniformly distributed load over the length of the castellated beam section under consideration. Three load locations were investigated: A) centered over the web post, B) centered over the hole, and C) centered mid-way between the center of the hole and the center of the web post. These load positions are identified as A, B and C and cover the potential concentrated load positions that

castellated beams will be subject to. The castellated beam section lengths for each of these three load cases are provided in Table 1 together with the aspect ratio between the section length,  $S$ , and the overall depth of the beam,  $d_g$ . The top flange of the castellated beam specimens was restrained against translations in directions 1 and 3 and against rotations about all three axis to simulate out-of-plane lateral bracing, the restraint provided by the rest of the beam and the restraint provided by the slab or any other supported member. The top flange was free to translate in the vertical direction to accommodate the application of the load. The bottom flange was restrained against all translations and rotations. The restraint provided by the continuation of the beam to the vertical edges of the webs was conservatively ignored and these edges were modeled as free. As stated above, the five selected beams were investigated for the case when their webs are unreinforced and reinforced with full height bearing stiffeners. The concentrated loads were assumed to apply over the supports. This loading arrangement is believed to be the most critical for the limit state of web post buckling, compared to other cases when the concentrated loads are applied away from the supports. 30 nonlinear finite element analysis were performed to obtain failure loads for the investigated specimens and to propose a simple design methodology that is based on the concept of an effective web width.

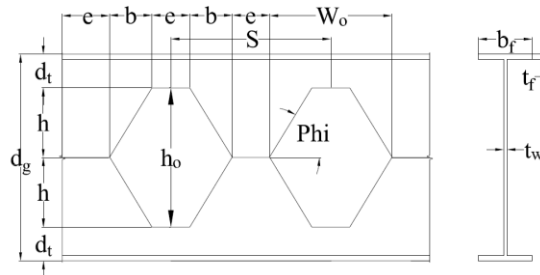
Table 1: Investigated castellated beams (CB)

W Section	CB Section	$h_{wcb}/t_w$	Section length ( $S^{**}$ ) (in.)		Aspect Ratio ( $S/d_g^{**}$ )	
			A*, B*	C*	A*, B*	C*
W8X40	CB12X40	25.6	11.5	5.75	1	0.50
W12X50	CB18X50	41.6	15.0	7.50	0.83	0.42
W16X50	CB24X50	59.8	19.0	9.50	0.77	0.39
W21X62	CB30X62	74.0	23.0	11.5	0.76	0.38
W27X84	CB40X84	86.6	30.0	15.0	0.74	0.37

\*Load position (Figure 8), \*\*See Table 2

Table 2: Geometry of investigated CBs

CB Section	e (in.)	b (in.)	$d_t$ (in.)	$d_g$ (in.)	$t_w$ (in.)	$b_f$ (in.)	$t_f$ (in.)	S (in.)	$h_o$ (in.)	h (in.)	$W_o$ (in.)	Phi (deg.)
CB12X40	4.0	1.75	2.50	11.5	0.375	8.125	0.563	11.5	6.50	3.25	7.50	61.70
CB18X50	4.5	3.25	3.25	18.0	0.375	8.125	0.625	15.0	11.375	5.75	10.75	60.27
CB24X50	4.5	5.00	4.00	24.5	0.375	7.125	0.625	19.0	16.50	8.25	14.50	58.81
CB30X62	6.0	5.50	6.00	30.0	0.375	8.250	0.625	23.0	18.00	9.00	17.00	58.54
CB40X84	7.0	8.00	6.50	40.5	0.438	10.00	0.625	30.0	27.375	13.75	23.00	59.74



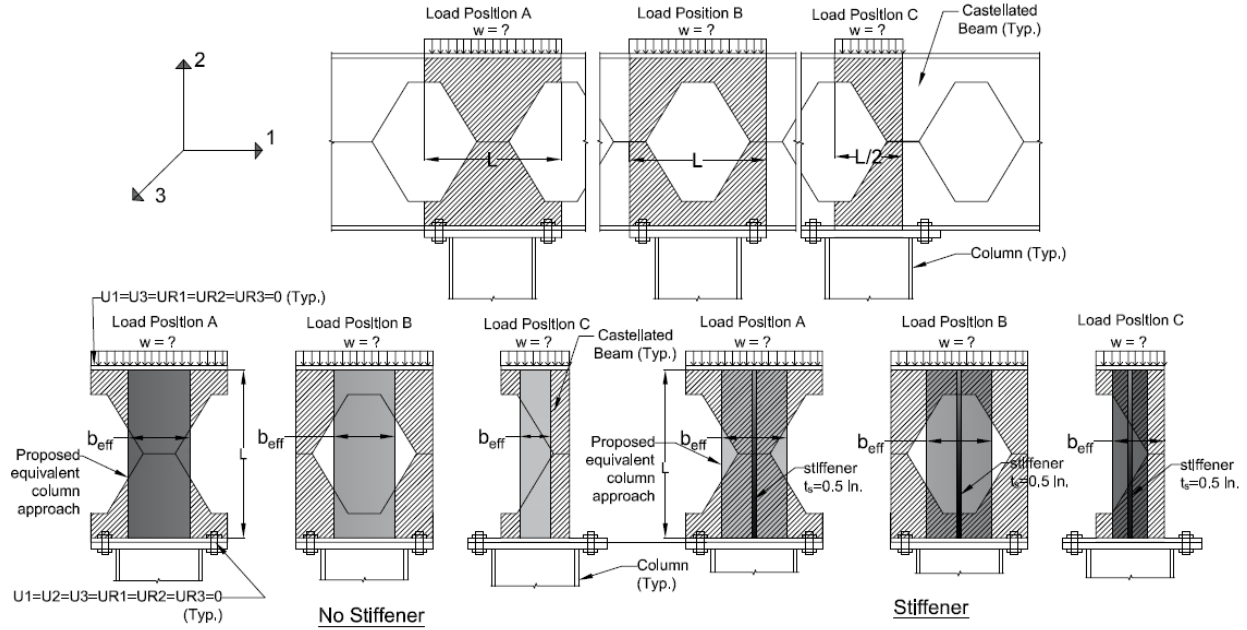


Figure 8: Investigated Cases

#### 4. Finite Element Analysis

The numerical simulations described in this paper were performed by using the commercially available finite element analysis software Abaqus (Dassault Systemes 2014). Because the primary goal of this investigation is the buckling of the web under concentrated loads, flanges were modeled as rigid bodies. The webs and stiffeners were modeled using S8R5 shell elements. The S8R5 element is a doubly-curved thin shell element with eight nodes and it employs quadratic shape functions. The “5” in S8R5 denotes that each element has five degrees of freedom (three translational, two rotational) instead of six (three translational, three rotational). The rotation of a node about the axis normal to the element mid-surface is removed from the element formulation to improve computational efficiency (Moen 2008). The “R” in the S8R5 designation denotes that the calculation of the element stiffness is not exact; the number of Gaussian integration points is reduced to improve computational efficiency and avoid shear locking (Moen 2008). This element is designed to capture the large deformations and through-thickness yielding expected to occur during the out-of-plane buckling of the web post to failure. The size of the mesh was selected such that each element side did not exceed 0.5 in. in length and was determined based on results from convergence studies to provide a reasonable balance between accuracy and computational expense. It was assumed that the self-weight of the specimens was negligible compared to the applied loads. Although the cross-section was symmetrical about the major and minor axis, it was necessary to model the full cross-section because the buckled shape could be non-symmetrical.

The finite element model takes into account both material and geometric nonlinearities. The structural steel was modeled using a bilinear stress strain relationship based on coupon test data provided by Arasaratnam et. al (2011). The true stress versus true strain relationship is shown in Figure 9 and was input into Abaqus to define the limits of the Von Mises yield surface. Young’s modulus  $E$ , was set at 29,000 *ksi* and Poisson’s ratio  $\nu$ , was set to 0.3. To initiate buckling, an initial small out-of-plane geometric imperfection, in the form of the first mode shape obtained from an eigenvalues buckling analysis, was imposed to the model. An Abaqus.fil file is created for each eigenbuckling analysis, which is then called from the nonlinear.inp file with the

\*IMPERFECTION command. During the design phase the imperfections are typically unknown and are accounted for in the design equations used to estimate the capacity of the members. They are usually used as general random quantities that can be rigorously treated by stochastic techniques (Soltani et al. 2012). In their investigation, Soltani et al. (2012) state that according to their knowledge, no consensus exists on maximum imperfection magnitudes for castellated beams even when the imperfection is in the shape of the lowest eigenmodes. Two imperfection magnitudes were used in the study performed by Soltani et al. (2012),  $d_w/100$  and  $d_w/200$ , where  $d_w$  is the clear web depth between the flanges, and it was shown that the model was not significantly affected by a change in the magnitude of the initial lateral deflection taken in the shape of the lowest buckling mode. Accordingly, the magnitude of the initial imperfection employed in this study is  $h_{cbw}/100$  (where  $h_{cbw}$  is the same as  $d_w$  used by Soltani et al.(2012)). Material nonlinearity is simulated in Abaqus with classical metal plasticity theory, including the assumption of a Von Mises yield surface. In this study residual stresses are not considered.

The modified Riks method was used to determine the nonlinear response of the castellated beam section. The modified Riks method (i.e., \*STATIC,RIKS in Abaqus), was developed in the early 1980's and enforces an arc length constraint on the Newton-Raphson incremental solution to assist in the identification of the equilibrium path at highly nonlinear points along the load-deflection curve (Crisfield 1981). The loads are applied uniformly along the length of the web and stiffeners when applicable. As stated above, top and bottom flanges were modeled as rigid bodies with reference nodes at the centroid of each flange (Figure 10). For each case the vertical displacement at the reference node of the top flange and the reaction at the reference node of the bottom flange were recorded. The maximum vertical displacement at the reference node of the top flange was typically limited to 2 in. because such a vertical displacement corresponded with loads that were much lower than the peak load and were well into the descending branch of the load displacement curve.

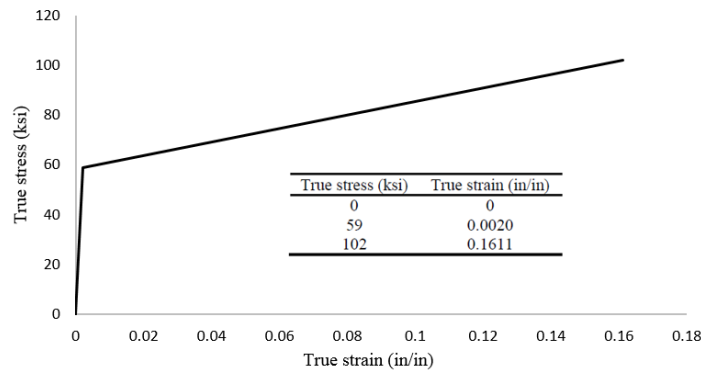


Figure 9: True stress-strain curve based on data from Arasaratnam et al. (2011)

## 5. Results

Figure 10 shows the first buckled mode shapes for CB12x40 when it is unreinforced and reinforced with stiffeners. As expected, the first buckled mode shape for the unreinforced cases is a typical out-of-plane buckling the castellated beam web. For the reinforced cases, the first buckled mode shape featured a combination of web and stiffener buckling for load cases A and C and only web buckling for load case B. This was due to the fact that although the stiffener in load case B was located such that it aligned with the center of the load, the web post was the weakest element and it buckled first. This behavior is similar to local buckling when in a given cross-section one element is more susceptible to buckling than the rest of the elements.

Figure 11 shows the deformed shape at simulated failure for all five cases investigated using CB12x40. As stated above, simulated failure corresponds to a vertical displacement of 2 in. in the reference node of the top flange. As expected, in all cases the deformed shape at failure is an exaggeration of the first buckled mode shape. Even for load case B when the section is reinforced with a stiffener, due to deformation compatibility, the stiffener is eventually engaged in the resistance against the applied load.

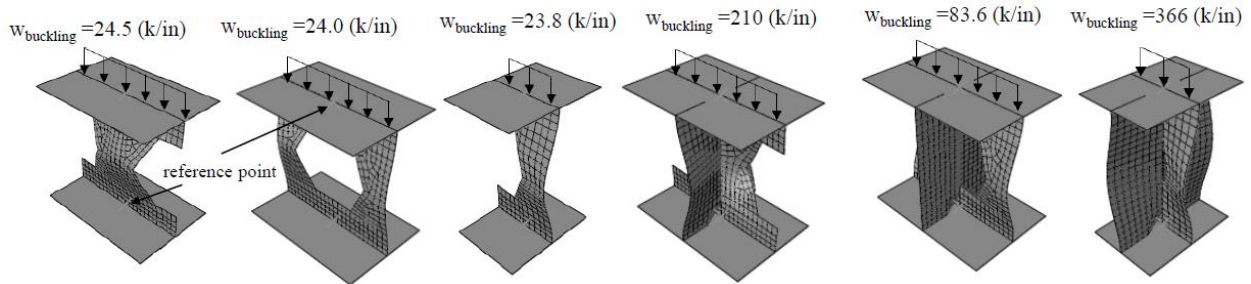
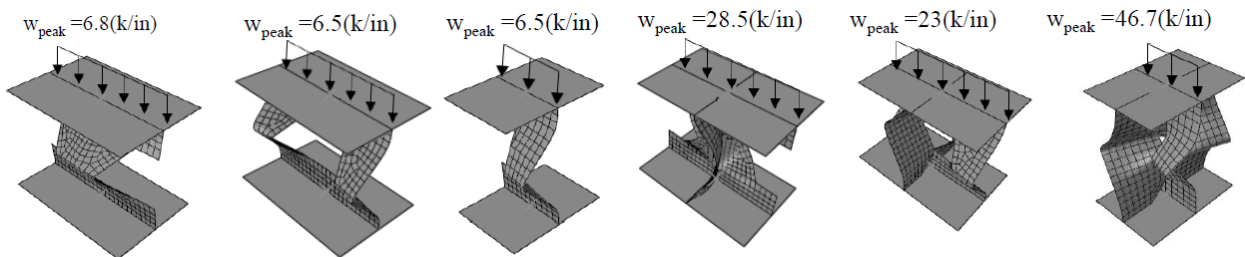


Figure 10: First buckled mode shape for CB12x40



Note: The deformed shape corresponds with a vertical deflection of 2 in. at the reference point of the top flange

Figure 11: Deformed shape at failure for CB12x40

Figure 12 illustrates the uniform load versus vertical displacement relationship for all investigated cases. Five graphs are presented with each graph illustrating the results pertaining to each castellated beam section. The uniform load is obtained by dividing the reaction obtained at the reference node of the bottom flange with the section length provided in Table 1. This was done to make a consistent comparison between all three load cases considered, given that the castellated beam section length for load case C is half of that considered in load cases A and B. The vertical displacement is obtained at the reference node of the top flange and the analysis was typically stopped when this value reached 2 in. As can be seen, all three unreinforced cases behaved similarly, and the load displacement curves are almost identical. This is expected and intuitive because the effective section resisting the applied load per unit length is the same. The peak uniformly distributed loads for each case are summarized in Table 3. It can be observed that for all cases the peak load decreases as the section depth increases. This is also expected and intuitive because the higher the unbraced length against buckling the lower the peak load.

The presence of stiffeners increases significantly the capacity of the castellated beam sections against concentrated loads. In almost all cases the highest resistance is provided by load case C when it is reinforced with a stiffener. This is due to the fact that even though the section length and the applied load were both half of those considered in cases A and B, the stiffener size was kept constant. Accordingly, reinforced load case C benefited relatively more from the presence of the stiffener. It can also be observed that the slope of the descending branch of the load displacement curve is smaller in reinforced load case A compared to reinforced load cases B and

C. This occurs because for load case A the stiffener was placed where it was needed the most, which is at the center of the web post. The center of the web post in all three cases is the section that is most susceptible to web buckling.

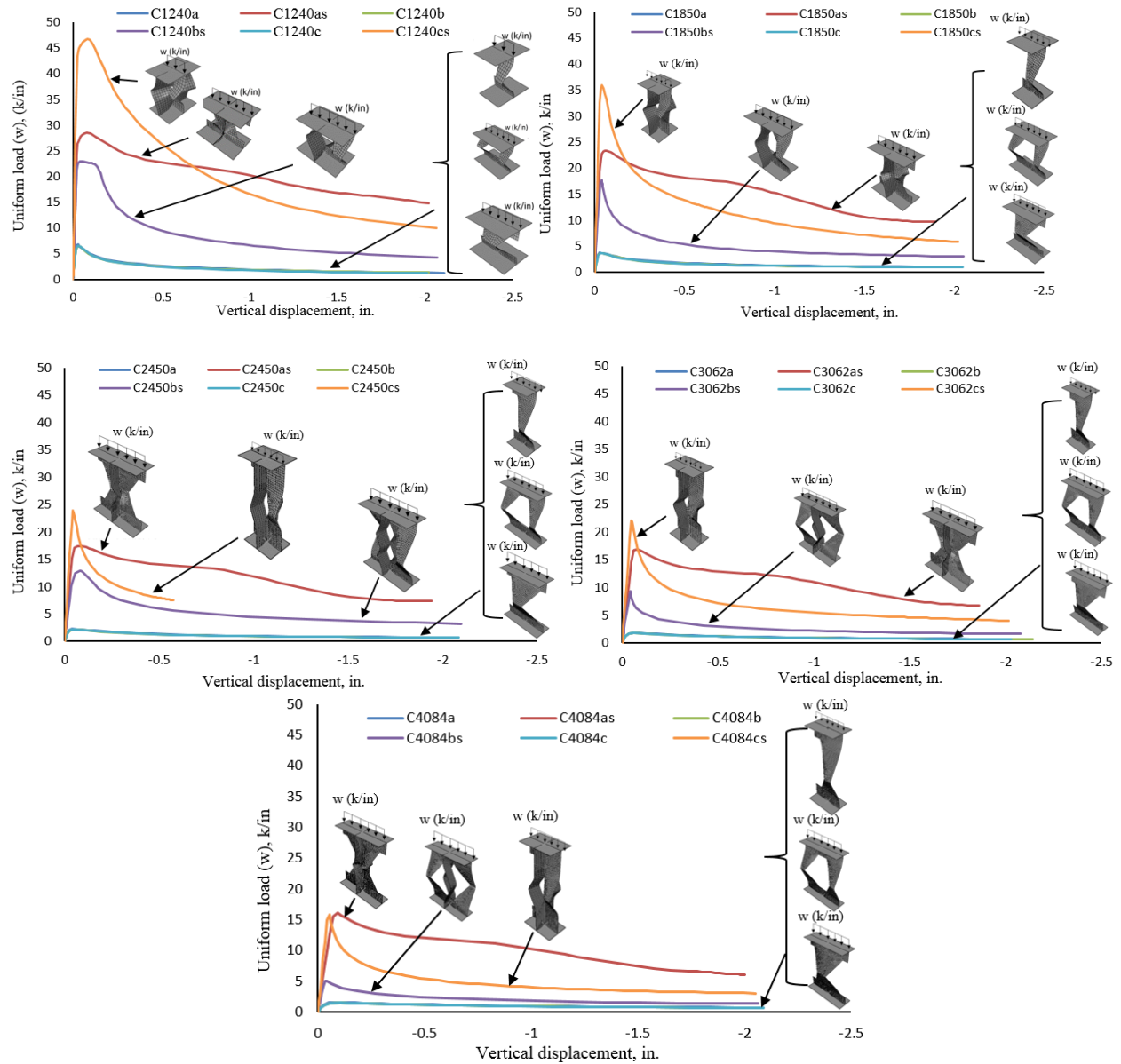


Figure 12: Uniform load versus vertical displacement at the top of the web post.

Table 3. Uniformly distributed failure load ( $w_n$  (k/in))

Load Position	C12x40		C18x50		C24x50		C30x62		C40x84	
	No stiff.	Stiffener								
A	6.8	28.5	3.7	23.3	2.3	17.4	1.8	16.9	1.6	16.0
B	6.5	23.0	3.6	17.7	2.2	12.9	1.8	9.4	1.5	5.0
C	6.5	46.7	3.6	35.9	2.2	24.0	1.8	22.0	1.5	15.9

The uniformly distributed load applied to the castellated beam sections was also normalized with respect to the uniformly distributed load that causes yielding at the smallest cross-section along the height of the web (mid-height of web) to investigate the efficiency of the sections in resisting the applied load (Figure 13). Figure 13 suggests that as the sections get deeper the effect of web slenderness becomes more pronounced in the unstiffened castellated beams. Also, in all stiffened cases and load position A the failure load is equal to or slightly higher than the yield load, which once again highlights the efficiency of the stiffener for this load position. The reason why in some cases the failure load is slightly higher than the yield load is attributed to strain hardening. In all cases the presence of the stiffeners enhances the capacity of the section significantly. Stiffened cases with load position C yielded lower ratios than those with load position A, but higher ratios than those with load position B. This again suggests the relative inefficiency of the stiffener location for load position B.

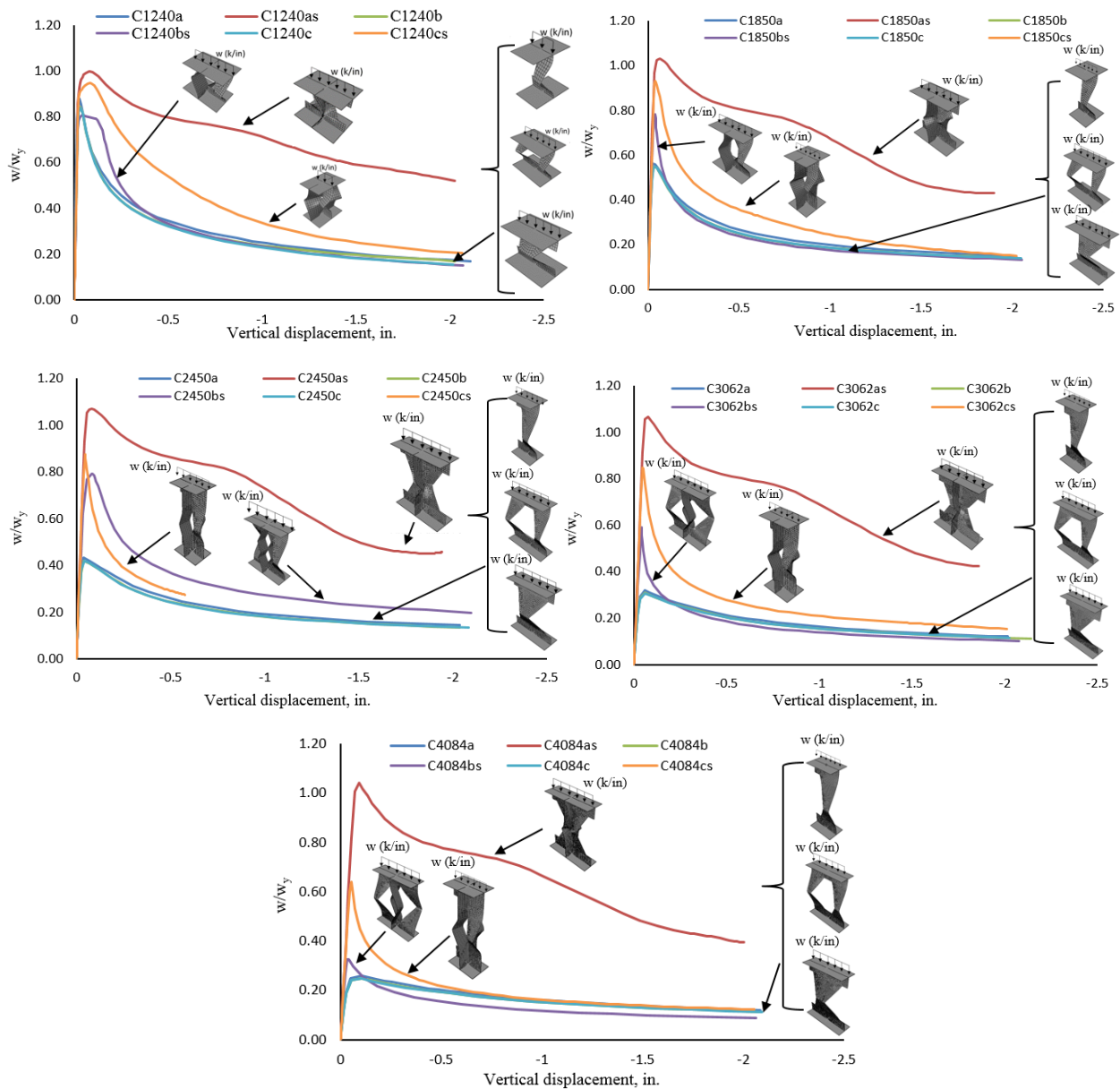


Figure 13: Normalized uniform load versus vertical displacement at the top of the web post.

The total reaction that corresponded with the peak load obtained at the reference point of the bottom flange was compared with the predicted nominal capacity of an equivalent solid web beam section calculated based on AISC Specifications (2010) Section J10. Only the unreinforced sections were included in this comparison and only articles J10.2 (web local yielding), J10.3 (web crippling) and J10.5 (web compression buckling) were considered because the investigated sections were adequately braced against out-of-plane translations at top and bottom flanges. The web local yielding provisions (Eq. 1 and 2) apply to both compressive and tensile forces of bearing and moment connections. These provisions are intended to limit the extent of yielding in the web of a member into which a force is being transmitted (AISC 2010). The bearing length  $l_b$ , in all cases was taken equal to the section length (Table 1) and  $k$  was taken as zero. The web crippling provisions (Eq. 3, 4 and 5) apply only to compressive forces, which is consistent with the cases investigated in this study. Web crippling is defined as crumpling of the web into buckled waves directly beneath the load, occurring in more slender webs, whereas web local yielding is yielding of that same area, occurring in stockier webs (AISC 2010). The web compression buckling provisions (Eq. 6 and 7) apply only when there are compressive forces on both flanges of a member at the same cross section, which is also consistent with the cases investigated in this study. Equation 6 is predicated on an interior member loading condition, and in the absence of applicable research, a 50% reduction has been introduced for cases wherein the compressive forces are close to the member end (Eq. 7) (AISC 2010). Equation 6 was developed by Chen and Newlin (1971) during a study on the column web buckling strength in beam-to-column connections. Equation 6 was derived by using the critical buckling stress of a square plate simply supported on all sides and by adjusting it to fit the results from the most critical test. Figure 14 shows the test setup. Because the investigation was focused on beam-to-column connections, Chen and Newlin state that from observations of the test results in the present and previous tests, it appears justified to assume that the concentrated beam-flange load acts on a square panel whose dimensions are  $d_c$  by  $d_c$ , where  $d_c$  is the column web depth.

In all cases, in which the load was assumed to be away from member ends, the limit state of web compression buckling controlled, with the exception of C12x40 load case C, in which web local yielding controlled over the other limit states. When the load was assumed to be at member ends, the limit state of web compression buckling controlled in all cases. Accordingly, this was primarily an evaluation of the applicability of Equations 6 and 7. Equations 6 and 7 used to predict web compression buckling in solid web beams are a function of web thickness ( $t_w$ ), modulus of elasticity ( $E$ ), web yield stress ( $F_{yw}$ ) and clear distance between flanges less the fillet ( $h$ ). Because these equations were derived assuming that the load is applied over a length equal to the depth of the web, they do not distinguish between various load bearing lengths.

Equation 6 grossly overestimated the nominal capacity of the castellated beam sections against concentrated loads when the loads were assumed to be away from the member ends. This was expected for several reasons. Equation 6 was developed for solid web beams and does not take into consideration the presence of the holes. Additionally, in the cases investigated in this study the restraint provided by the continuation of the castellated beam to the web on both sides (if applicable) was conservatively ignored, whereas in the derivation of Equation 6 the square web panel was assumed to be simply supported on all sides. Also, the aspect ratio between the loaded length and member depth was at best 1.0 (Table 1).

When the load was assumed to be at member ends (Eq. 7), the prediction improved, especially for load cases A and B. This is also expected, because when the load is applied at member ends the restraint provided by the continuation of the castellated beam to the web applies only to one

end and it represents more closely the boundary conditions used in this study. For load case C the equation still grossly overestimated the capacity of the castellated beam sections because it does not take into account the shorter loaded length and the lower aspect ratios.

The average between the peak load obtained from nonlinear finite element analysis and that obtained from the AISC web buckling provisions assuming that the load is at member ends, was 1.16 for load position A and B, and 0.57 for load position C.

**Web Local Yielding**

*Away from member ends*

$$R_n = F_{yw}t_w(5k + l_b) \quad (1)$$

*At member ends*

$$R_n = F_{yw}t_w(2.5k + l_b) \quad (2)$$

where

$t_w$  = web thickness, in.

$F_{yw}$  = web yield stress (59 ksi)

$k$  = distance from outer face of the flange to the web toe of the fillet, in.

$l_b$  = length of bearing, in.

**Web Local Crippling**

*Away from member ends*

$$R_n = 0.80t_w^2 \left[ 1 + 3 \left( \frac{l_b}{d} \right) \left( \frac{t_w}{t_f} \right)^{1.5} \right] \sqrt{\frac{EF_{yw}t_f}{t_w}} \quad (3)$$

*At member ends*

*for  $l_b/d \leq 0.2$*

$$R_n = 0.40t_w^2 \left[ 1 + 3 \left( \frac{l_b}{d} \right) \left( \frac{t_w}{t_f} \right)^{1.5} \right] \sqrt{\frac{EF_{yw}t_f}{t_w}} \quad (4)$$

*for  $l_b/d > 0.2$*

$$R_n = 0.40t_w^2 \left[ 1 + \left( \frac{4l_b}{d} - 0.2 \right) \left( \frac{t_w}{t_f} \right)^{1.5} \right] \sqrt{\frac{EF_{yw}t_f}{t_w}} \quad (5)$$

where

$E$  = modulus of elasticity (29000 ksi)

$d$  = full nominal depth of the section, in.

$t_f$  = thickness of flange, in.

**Web Compression Buckling**

*Away from member ends*

$$R_n = \frac{24t_w^3 \sqrt{EF_{yw}}}{h} \quad (6)$$

*At member ends*

$$R_n = \frac{12t_w^3 \sqrt{EF_{yw}}}{h} \quad (7)$$

where

$h$  = clear distance between flanges less the fillet

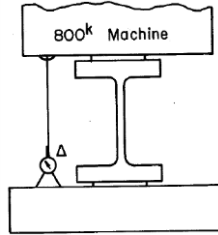


Figure 14: Test setup used by Chen and Newlin to investigate web buckling strength (1971)

Table 4. Comparison of predicted failure loads

Load Position	FEA <sup>1</sup> (kips)	AISC <sup>2</sup> (kips)		Ratio = FEA/AISC	
		Away from member ends	At member ends	Away from member ends	At member ends
C12x40	A	77.8	172.6	0.45	0.90
	B	74.6	172.6	0.43	0.86
	C	37.2	127.2 <sup>3</sup>	0.29	0.43
C18x50	A	56.0	105.3	0.53	1.06
	B	54.6	105.3	0.52	1.04
	C	27.2	105.3	0.26	0.52
C24x50	A	43.1	73.8	0.58	1.17
	B	41.7	73.8	0.57	1.13
	C	20.8	73.8	0.28	0.56
C30x62	A	42.3	59.6	0.71	1.42
	B	41.0	59.6	0.69	1.38
	C	20.4	59.6	0.34	0.68
C40x84	A	47.1	69.2	0.68	1.36
	B	45.1	69.2	0.65	1.30
	C	22.5	69.2	0.33	0.65
Average of A and B					1.16
Average of C					0.57

<sup>1</sup>Nominal capacity computed from nonlinear finite element analysis

<sup>2</sup>Nominal capacity calculated based on AISC Sections J10.2, J10.3 and J10.5. Typically governed by J10.5 (web compression buckling unless otherwise noted)

<sup>3</sup>Governed by web local yielding

## 6. Proposed Simplified Approach

The results from nonlinear finite element analysis were used to calculate an effective web width for castellated beams with and without bearing stiffeners. This effective web width will allow the engineers to check the limit state of web buckling due to compression by treating unstiffened webs as rectangular columns and stiffened webs as columns with a cruciform cross-sectional shape (Figure 15). The capacity of these equivalent columns can then be calculated based on AISC Specifications (2010). The equivalent rectangular column can be designed in accordance with AISC Specifications Section E3 and the equivalent column with the cruciform cross-sectional shape can be designed in accordance with Sections E3 and E4. In this approach, the effects of local buckling for the cruciform cross-sectional shape need not be considered because the effective width was computed to match the results from nonlinear finite element analysis, which account for local buckling effects. The height of the equivalent columns is taken equal to clear height of the web ( $h_{web}$ ) of the castellated beam. This height is different from that used in design approaches proposed by other investigators (Blodgett 1966; United Steel Co. Ltd. 1957 and 1962; and Hosain and Speirs 1973), in which the height of the column was taken equal to clear height of the hole. After examining the deformed shapes of the castellated beam sections at simulated failure, it was

decided to take  $K$  equal to 0.5. Table 5 provides a summary of the effective web widths for all the investigated cases.

For the unstiffened cases the effective width typically increases as the castellated beam depth increased. Also, for the stiffened cases and load position A the effective width increased as the section depth increases, however for load positions B and C there was no direct relationship between the increase in depth and the magnitude of the effective web width.

In most unstiffened cases, the calculated effective width is greater than the minimum width of the castellated beam web post  $e$  (see Table 2). For all stiffened cases and load position A the effective widths are always greater than  $e$ . For stiffened cases in which load position B was investigated, the effective width was always smaller than  $e$ , and for stiffened cases and load position C the effective width was greater than  $e$  for C12x40, C18x50, C24x50 and smaller than  $e$  for C30x62 and C40x84. The reason why in some of the stiffened cases the effective width was smaller than  $e$ , is attributed to the fact that the loads obtained from nonlinear finite element analyses include the effects of local buckling and the proposed approach was developed such that the engineer would only have to check the global buckling of the equivalent column shapes. The results provided in Table 6 suggest once again that the stiffeners in load case B are not placed in the optimal position, because the buckling of the web post occurs prior to the efficient engagement of the stiffeners.

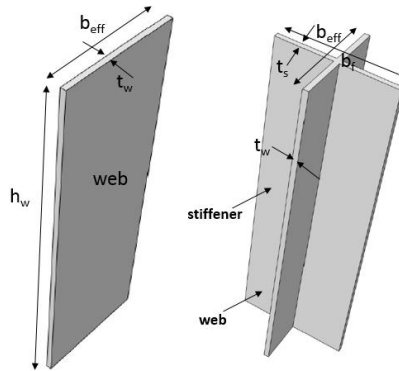


Figure 15: Equivalent rectangular and cruciform column sections

Table 5: Effective Web Width ( $b_{eff}$  (in.)) ( $K=0.5$ )

Load Position	C12x40		C18x50		C24x50		C30x62		C40x84	
	No stiff.	Stiffener								
A	4.29	5.63	4.24	7.48	5.28	7.74	7.93	12.17	10.36	13.28
B	4.11	2.37	4.14	2.63	5.11	2.70	7.68	2.11	9.91	1.86
C	2.05	2.58	2.06	2.84	2.55	2.30	3.82	2.58	4.94	2.38

Table 6: Comparison of effective web width with minimum width of web post (K=0.5)

Section	Stiffener	Load Position	$b_{eff}^*$ (in.)	$e^{**}$ (in.)	Section width ( $S^{**}$ ) (in.)	Ratio= $b_{eff}/e$
C12x40	No	A	4.29	4.00	11.5	1.07
		B	4.11	4.00	11.5	1.03
		C	2.05	2.00	5.75	1.03
	Yes	A	5.63	4.00	11.5	1.41
		B	2.37	4.00	11.5	0.59
		C	2.58	2.00	5.75	1.29
C18x50	No	A	4.24	4.25	15	1.00
		B	4.14	4.25	15	0.97
		C	2.06	2.125	7.5	0.97
	Yes	A	7.48	4.25	15	1.76
		B	2.63	4.25	15	0.62
		C	2.84	2.125	7.5	1.34
C24x50	No	A	5.28	4.50	19	1.17
		B	5.11	4.50	19	1.14
		C	2.55	2.25	9.5	1.13
	Yes	A	7.74	4.50	19	1.72
		B	2.70	4.50	19	0.60
		C	2.30	2.25	9.5	1.02
C30x62	No	A	7.93	6.00	23	1.32
		B	7.68	6.00	23	1.28
		C	3.82	3.00	11.5	1.27
	Yes	A	12.17	6.00	23	2.03
		B	2.11	6.00	23	0.35
		C	2.58	3.00	11.5	0.86
C40x84	No	A	10.36	7.00	30	1.48
		B	9.91	7.00	30	1.42
		C	4.94	3.50	15	1.41
	Yes	A	13.28	7.00	30	1.90
		B	1.86	7.00	30	0.27
		C	2.38	3.50	15	0.68

\*See Figure 8, \*\*See Table 2

## 7. Conclusions

The research presented in this paper addressed the need for a design method to estimate the nominal capacity of castellated beams against concentrated loads. The limit state investigated in this study was that of web post buckling due to compression loads. Five castellated beam section depths were considered which cover a wide range of the available depths. For each section three load cases were considered: A) center of load aligns with the middle of web post, B) center of load aligns with the center of the hole, and C) center of load aligns with a point half-way between the center of web post and center of hole. For each load position two cases were considered; one without a stiffener and one with a full height stiffener. This resulted in a total of 30 cases, which were investigated using nonlinear finite element analyses that accounted for geometric and material nonlinearities including the effect of initial imperfections.

The peak loads obtained from the analyses of unstiffened cases were compared with AISC provisions for flanges and solid webs with concentrated forces. Only Sections J10.2, J10.3 and J10.5 were considered for comparison because the castellated beam sections were assumed to be adequately braced for out of plane translations at the top and bottom flanges. When the load was

considered to be away from member ends, AISC provisions for solid web beams grossly overestimated the capacity of the sections under consideration. This was expected for several reasons. Equation 6 was developed for solid web beams and does not take into consideration the presence of the holes. Additionally, in the cases investigated in this study the restraint provided by the continuation of the castellated beam to the web on both sides (if applicable) was conservatively ignored, whereas in the derivation of Equation 6 the square web panel was assumed to be simply supported on all sides. Also, the aspect ratio between the loaded length and member depth was at best 1.0 (Table 1). When the load was assumed to be at member ends (Eq. 7), the prediction improved, especially for load cases A and B. This is also expected, because when the load is applied at member ends the restraint provided by the continuation of the beam to the web applies only to one end and it represents more closely the boundary conditions used in this study. For load case C the equation still grossly overestimated the capacity of the castellated beam sections because it does not take into account the shorter loaded length and the lower aspect ratios. The average between the peak load obtained from nonlinear finite element analysis and that obtained from the AISC web buckling provisions assuming that the load is at member ends, was 1.16 for load position A and B, and 0.57 for load position C.

A simplified approach was presented for checking the limit state of web post buckling in compression, which considers the web of a castellated beam as an equivalent column whose height is equal to the clear height of the web. For the unstiffened cases the equivalent column has a rectangular cross-section whose thickness is equal to the thickness of the web and the width can be determined based on the effective width values presented in this paper. This equivalent rectangular column can be checked using AISC (2010) provisions in Section E3. For the stiffened case the equivalent column has a cruciform cross-sectional shape that consist of the beam web and the stiffener. The width of the castellated beam web than can be used to determine the capacity of the column can be determined based on the effective width values presented in this paper. The equivalent column with a cruciform cross-sectional shape need only be checked for global buckling using the provisions of AISC Specifications (2010) in Sections E3 and E4, because the effects of local buckling were included in the calculation of the effective web width. A K value equal to 0.5 is recommended based on an examination of the deformed shapes of castellated beam sections at simulated failure.

The capacity of the unstiffened beams against concentrated loads as it relates to the limit state of buckling of the web post in compression, ranged from 1.5 k/in to 6.8 k/in assuming that the load was applied over a distance equal to the spacing of the holes for load cases A and B and half the distance between the holes for load case C. These capacities were significantly increased when the castellated beam sections were reinforced with stiffeners and they ranged from 5 k/in to 47 k/in. These values together with the results presented in this paper can be used to determine the necessity of stiffeners in castellated beams to prevent the buckling of the web post due to compression.

## References

- Abaqus User's Manual Version 6.14-2, Dassault Systemes Simulia Corp. (2014).
- AISC (2010), "Specification for Structural Steel Buildings", AISC, Chicago, IL.
- Arasaratnam, P., Sivakumaran, K. S., & Tait, M. J. (2011), "True stress-true strain models for structural steel elements", *International Scholarly Research Notices*.
- Blodgett, O. W. (1966). Design of welded structures. Cleveland: James F. Lincoln Arc Welding Foundation, 1966, 1.
- Chen, F. W., Newlin, D. E., "Column Web Strength in Steel Beam-to-Column Connections", ASCE Annual and National Environmental Engineering Meeting October 18-22, 1971, St. Louis, Missouri.
- Crisfield, M.A. (1981). "A fast incremental iteration solution procedure that handles snapthrough," *Computers and Structures*, 13, 55-62.
- Darwin, D., (2003), Steel Design Guide 2, "Steel and Composite Beams with Web Openings", AISC, Chicago, IL.
- ENV 1993-1-1, (1993) Eurocode 3: Design of steel structures-Part 1-1: general rules and rules for buildings, 1992, and amendment A2 of Eurocode 3: Annex N 'Openings in Webs'. British Standards Institution; 1998.
- "Design of composite beams with large openings for services", (2006), *The Steel Construction Institute publication document RT959 version 05*; May.
- Durif, S., Bouchair, A., and Vassart, O. (2013), "Experimental tests and numerical modeling of cellular beams with sinusoidal openings", *Journal of Constructional Steel Research*, 82, 72-87.
- Ellobody, E. (2011), "Interaction of buckling modes in castellated steel beams", *Journal of Constructional Steel Research*, 67(5), 814-825.
- Ellobody, E. (2012), "Nonlinear analysis of cellular steel beams under combined buckling modes", *Thin-Walled Structures*, 52, 66-79.
- Halleux, P., Etude experimentale et technique du comportement elastique des poutres metalliques / time 6vid6e, *Revue Française de Mecanique, Memoires du Groupement pour l'A vancement des Methodes d'Analyse des Contraintes*, 18 et 19 (1966) 123-40
- Halleux, P., "Limit analysis of castellated steel beams", *Acier-Stahl-Steel*, 32, No. 3 (March 1967) 133--44.
- Hosain, M. U., and Spiers, W. G. (1973), "Experiments on castellated steel beams", *Supplement to Welding Journal*, American Welding Society and the Welding Research Council.
- Nethercot, D. A. and Kerdal, D., "Lateral-torsional buckling of castellated beams", *The Structural Engineer*, 60B, No. 3 (September 1982) 53-61.
- Kerdal, D., and Nethercot, D. A. (1984), "Failure modes for castellated beams", *Journal of Constructional Steel Research*, 4(4), 295-315.
- Moen, D.C., (2008), "Direct strength design of cold-formed steel members with perforations", *PhD Dissertation*, John Hopkins University, Baltimore, MD.
- Scherer Steel Structures, Inc., <http://scherersteel.com/joists-girders/image001/>
- Soltani, M. R., Bouchair, A., Mimoune, M. (2012), "Nonlinear FE analysis of the ultimate behavior of steel castellated beams", *Journal of Constructional Steel Research*, 70, 101-114.
- Wang, P., Ma, Q., & Wang, X. (2014), "Investigation on Vierendeel mechanism failure of castellated steel beams with fillet corner web openings", *Engineering Structures*, 74, 44-51.
- Tsavdaridis, K. D., & D'Mello, C. (2011), "Web buckling study of the behaviour and strength of perforated steel beams with different novel web opening shapes", *Journal of Constructional Steel Research*, 67(10), 1605-1620.
- Tsavdaridis, K. D., D'Mello, C. (2012). Optimisation of novel elliptically-based web opening shapes of perforated steel beams. *Journal of Constructional Steel Research*, 76, 39-53.
- United Steel Co. Ltd., Res. and Dev. Dep., "Properties and strengths of castella beams", (1957) Consideration of previous tests', Report D.GE. 71/262, Swinden Laboratories, Rotherham, April.
- United Steel Co. Ltd., Res. and Dev. Dept., "Web strength of castella beams", (1962) Report D.TS. 6/262/6, Swinden Laboratories, Rotherham, May.
- Zaarour, W., & Redwood, R. (1996), "Web buckling in thin webbed castellated beams. *Journal of structural engineering*", 122(8), 860-866.